IEEE Access
Multidisciplinary ⋮ Rapid Review ⋮ Open Access Journal

Received 9 May 2024, accepted 3 July 2024, date of publication 15 July 2024, date of current version 24 July 2024.

Digital Object Identifier 10.1109/ACCESS.2024.3428356

RESEARCH ARTICLE

Exploiting Zero Forcing and Block Diagonalization Precoding for Multi-User MIMO ISAC: Bridging Communications and Sensing

CARLOS RAVELO[1], (Graduate Student Member, IEEE), DAVID MARTÍN-SACRISTÁN[1], AND JOSE F. MONSERRAT[2], (Senior Member, IEEE)

[1]5G Communications for Future Industry Verticals, 46022 Valencia, Spain
[2]iTEAM Research Institute, Universitat Politècnica de València, 46022 Valencia, Spain

Corresponding author: Carlos Ravelo (carlos.ravelo@fivecomm.eu)

This work was supported in part by the MSCA within the H2020 Framework under Project 955629 ITN-5VC.

ABSTRACT This paper explores the potential of applying Zero Forcing (ZF) and Block Diagonalization (BD), two linear precoding techniques commonly utilized in communications, to a Multi-User Multiple Input Multiple Output (MU-MIMO) Integrated Sensing and Communications (ISAC) setup. The parallels between communications and sensing are highlighted to show the feasibility of extending ZF and BD to ISAC. To enable the implementation of these techniques, the concept of sensing channel is exploited, enabling the treatment of the sensing receiver as an additional user. Furthermore, two user selection strategies extend existing communication-only algorithms to accommodate sensing requirements. The efficacy of the proposed techniques is substantiated through comprehensive simulations. With the proposed solution, a high beampattern gain is maintained for the sensing while keeping good communication performance, only limited by the power allocation between the two functionalities.

INDEX TERMS ISAC, MU-MIMO, precoding, user selection.

I. INTRODUCTION

Integrated Sensing and Communications (ISAC) has recently received considerable attention from both the research community and the industry, motivated by the possibility of exploiting the spectrum more efficiently and achieving integration gains for communications and sensing. The joint operation of these two functionalities, which have traditionally been developed separately, has been extensively studied on different integration levels, from coexistence to complete redesign of current systems with architectures conceived with ISAC as a core component. While coexistence would be easier to implement, it would not provide the same performance gains as a joint design, so most literature focuses on the latter. Comprehensive analyses of the state of the art in the topic can be found in [1] and [2].

The implementation of ISAC in mobile networks has understandably been one of the most studied topics in the related literature, and authors believe that sensing will be a fundamental part of 6G [2], [3], [4], [5]. Given the evolution of wireless technologies, a convergence of communications and radar can be seen, supporting the development of ISAC solutions. The need for more bandwidth and the exploitation of Multiple-Input Multiple-Output (MIMO) techniques are examples of the similarities between radars and mobile networks that suggest ISAC is becoming increasingly feasible. An excellent overview of ISAC for mobile networks is given in [6].

Ultimately, sensing would be a new network functionality, offering a valuable opportunity to support new use cases and services. The sensing receiver could be added to existing

The associate editor coordinating the review of this manuscript and approving it for publication was Luyu Zhao.

transceivers, and adequate adaptations to current processing chains would enable reusing communication functionalities to benefit sensing. While early studies on ISAC consider mainly Single Input Single Output (SISO) setups [7], [8], the extension to MIMO has been included in more recent works. As mobile networks have matured to implement Multi-User MIMO (MU-MIMO), it is reasonable to expect that ISAC can be deployed in such setups, adding the sensing receiver as another user with its specific requirements. The need to serve communication users and perform sensing simultaneously opens up problems such as resource allocation optimization and the design of precoding strategies. In the literature, multiple studies of optimality within MU-MIMO ISAC setups can be found, tackling the problem from different directions like optimal waveform design [9] and precoder optimization [10], [11].

In [9], the design of an optimal waveform for ISAC is studied on a MIMO radar setup, considering both the target detection stage, where omnidirectional probing is performed, and the design of a directional radar beam pattern for tracking targets. The waveform is obtained by solving optimization problems in which the multi-user interference between communication users is minimized. The initial problems are later adjusted to control the trade-off between communications and radar performance, and an efficient algorithm is proposed to find the solution. In [10], the optimization is done to minimize the Cramer-Rao Lower-Bound (CRLB) on the Angle of Arrival (AoA) estimation of the target's echoes while maintaining the Signal-to-Interference-plus-Noise Ratio (SINR) over a predefined threshold for all communication users. The authors solve the problem for the point-scatter and the extended target models by applying semi-definite relaxation to the initially non-convex problems. In [11], the multi-antenna transmitter is designed to have a covariance matrix equal to an optimal covariance for MIMO radar. Additionally, Dirty Paper Coding (DPC) cancels the interference across communication users.

In these works, the solutions are found through solving optimization problems. However, this approach can be computationally prohibitive for real-time applications, especially as the number of users grows. While in [9], it is mentioned that a closed-form solution to the omnidirectional beam pattern problem could be reached by applying Zero-Forcing (ZF), the introduction of the modified optimization problem with a term controlling the trade-off between the two functions negates this option. This paper considers an alternative approach, extending linear precoding methods initially developed for communications-only scenarios to include the sensing functionality.

We study a scenario in which a Base Station (BS) transmits multiple data streams for communication users and one stream for sensing in an MU-MIMO fashion. Supporting the idea of sensing and communications convergence, we treat a monostatic sensing receiver at the BS as an additional user and apply ZF beamforming for the single-antenna communication users case and Block-Diagonalization (BD) for the extension to multi-antenna users. Since MU-MIMO usually requires Channel State Information at the Transmitter (CSIT), the estimation of the sensing channel is a necessary step to be able to reduce interference between communications and sensing. The sensing channel can be understood as the effects of scatterers surrounding the ISAC capable BS, including targets, and we consider that its estimation has been done by periodically transmitting unprecoded pilots. Using the same precoding algorithms for sensing and communications allows the reuse of functional blocks, easing the integration. While the proposed methods can be used with multiple waveforms, we will consider the use of Orthogonal Frequency Division Multiplexing (OFDM), which has been extensively studied as ISAC waveform [7], [12], [13]. In our analysis, we consider both target detection and target tracking stages of sensing and demonstrate that, while the goal in both cases can be equated to maximizing the SINR in the sensing receiver, the different requirements of both stages can influence the power allocation. The main limitation of the proposed method is the need to use fully digital precoding and the costs of hardware complexity and power consumption that it might imply. We leave alternate methods like hybrid beamforming for future work. Additionally, while we are considering perfect CSIT, the case for partial CSIT or evaluating the influence of imperfect CSIT is left for future work.

The contributions of the paper can be summarized as follows:

- The adaptations for ZF beamforming and BD to be applied in a MU-MIMO ISAC setting are presented. In addition to the classical precoding for the downlink channel, we explain the required decoding to eliminate interference in the sensing receiver. We show how, by using the Line of Sight (LoS) channel to a sensing location or target as a starting point for the sensing beamforming, ZF and BD are directly applicable for MU-MIMO in ISAC.
- Two algorithms for user selection are introduced, based on existing user selection algorithms for communication, extending them to ISAC. To our knowledge, the user selection problem has not been previously considered for ISAC.

The paper is organized as follows: Section II presents the system model. In Section II-A, a brief review of the used OFDM ISAC processing method is given, and in Section II-B, the performance metrics that will be considered in the proposed solutions are presented. Next, Section III describes the proposed linear processing algorithms, highlighting the modifications to the typical communication-only scenario and presenting the optimization of the joint performance in Section III-C. Section IV delves into the user selection problem for ISAC, and Section V presents the results of simulations. Finally, Section VI draws the main conclusions of the paper.

The following conventions are followed throughout the paper: bold lowercase letters represent vectors, and bold

uppercase letters represent matrices. The $(\cdot)^*$ operator denotes the conjugate transpose of a matrix, while $(\cdot)^T$ represents its transpose, det$(\cdot)$ represents its determinant, and $|\cdot|$ is the absolute value. Alternatively, when referring to a set $|\cdot|$ represents its cardinality. The symbols $\vee$ and $\wedge$ represent the logical or and logical and operations, respectively.

II. SYSTEM MODEL

We consider an In-Band Full-Duplex (IBFD) capable BS with N_t transmitting antennas that is serving $U < N_t - 1$ communication users through a MU-MIMO broadcast channel and, at the same time, it is sensing the environment using OFDM as ISAC waveform. The sensing will be performed by scanning in pre-configured directions that could have been determined by a beam planning strategy in the case of target detection or by pointing the beam towards the estimated position of a previously detected target in the case of tracking. For this paper, we will consider that only one sensing direction is served alongside U communication users and that the multiple sensing locations or targets are multiplexed in orthogonal time/frequency resources. This consideration can be justified by the poor spatial orthogonality that could exist between multiple targets which need to be on LoS with respect to the BS, and with positions confined within a restricted space like is the case of vehicles on the street. We will consider that the U users have the same number of receiving antennas N_r, and the BS will send $N_s = N_r$ streams to each one. The data sent to the u-th user, $\mathbf{s}_u$, will be precoded by the matrix $\mathbf{F}_u \in \mathbb{C}^{N_t \times N_s}$, where N_t is the number of transmitting antennas. At the same time, the BS sends a sensing stream s_s towards the sensed location, precoded by the vector $\mathbf{f}_s \in \mathbb{C}^{N_t \times 1}$. The signal, $\mathbf{x} \in \mathbb{C}^{N_t \times 1}$, sent on the n-th subcarrier and m-th symbol of the transmitted OFDM grid is given by

$$\mathbf{x}^{(n,m)} = \sum_{u=0}^{U-1} \sqrt{\frac{P_u}{N_t}} \mathbf{F}_u^{(n,m)} \mathbf{s}_u^{(n,m)} + \sqrt{\frac{P_s}{N_t}} \mathbf{f}_s^{(n,m)} s_s^{(n,m)}, \tag{1}$$

where P_u, P_s represent the power allocated to the data stream of the u-th user and sensing stream respectively, and need to fulfill

$$\sum_{u=0}^{U-1} P_u + P_s \leq P_t, \tag{2}$$

with P_t representing the total transmit power. The superscripts $^{(n,m)}$ on (1) stem from the fact that the precoders are dependent on the channel estimation obtained in advance (e.g., through uplink pilots), which varies across time and frequency. We will consider fully digital precoders, leaving the case of hybrid beamforming for future work. For ease of representation, in the following, we will omit the superscripts, and the reader can assume the analysis is done on the OFDM grid domain unless indicated otherwise.

At the u-th communication user, the received signal at the N_r antennas, $\mathbf{y}_u \in \mathbb{C}^{N_r \times 1}$, is given by

$$\mathbf{y}_u = \sqrt{G_u} \mathbf{H}_u \mathbf{x} + \mathbf{z}_u, \tag{3}$$

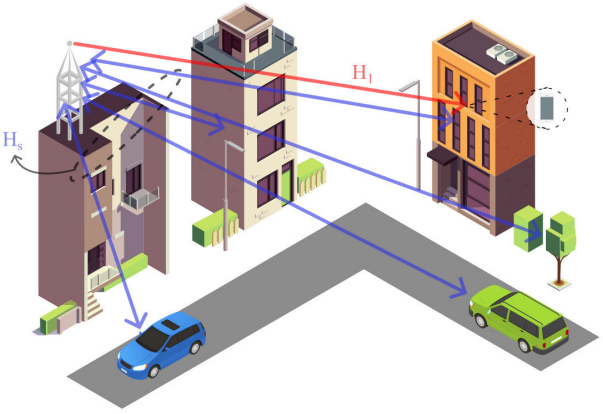

FIGURE 1. Communications and sensing channels.

where $\mathbf{H}_u \in \mathbb{C}^{N_r \times N_t}$ is the normalized channel between the BS and the communication user, with gain G_u, and $\mathbf{z}_u$ is the received noise which we will consider zero-mean circularly symmetric white Gaussian. After applying a decoding matrix $\mathbf{D}_u \in \mathbb{C}^{N_s \times N_r}$ to separate the N_s streams we end up with the received symbol

$$\tilde{\mathbf{y}}_u = \mathbf{D}_u \mathbf{y}_u. \tag{4}$$

Combining (1), (3) and (4), we can obtain the following expression for the decoded signal where we have conveniently grouped, in this order, the terms related to the useful information, the interference from other communication signals, the interference from the sensing signal, and the noise after the decoding process $\tilde{\mathbf{z}}_u$.

$$\tilde{\mathbf{y}}_u = \sqrt{\frac{G_u P_u}{N_t}} \mathbf{D}_u \mathbf{H}_u \mathbf{F}_u \mathbf{s}_u + \sum_{j=0, j\neq u}^{U-1} \sqrt{\frac{G_u P_j}{N_t}} \mathbf{D}_u \mathbf{H}_u \mathbf{F}_j \mathbf{s}_j + \sqrt{\frac{G_u P_s}{N_t}} \mathbf{D}_u \mathbf{H}_u \mathbf{f}_s s_s + \tilde{\mathbf{z}}_u. \tag{5}$$

The analysis of the sensing receiver can be done considering the sensing channel $\mathbf{H}_s \in \mathbb{C}^{N_t \times N_t}$. This matrix models the effect of the channel on the sensing signals transmitted from the BS since they leave the BS until their echoes reach the sensing receiver at the BS again. The total effect includes both the interaction of the signal with the sensing target and with other elements surrounding the BS. In Fig. 1 the communication and sensing channels are represented. The communications channel gathers the influence of scatterers from the BS to the User Equipment (UE)s while the sensing channel is determined by the influence of scatterers in the path from the transmitter to the sensing receiver, which in this case is colocated. For clarity, only single-hop scatterer reflections have been represented.

The signal received at the sensing receiver, $\mathbf{y}_s \in \mathbb{C}^{N_t \times 1}$, is given by

$$\mathbf{y}_s = \sqrt{G_s} \mathbf{H}_s \mathbf{x} + \mathbf{z}_s. \tag{6}$$

After applying the decoding vector $\mathbf{d}_s \in \mathbb{C}^{1\times N_t}$ we obtain the decoded symbol, y_s, formed by three terms related to useful sensing signal, interference from communication streams and noise $\tilde{z}_s$, respectively:

$$\tilde{y}_s = \sqrt{\frac{G_s P_s}{N_t}}\mathbf{d}_s\mathbf{H}_s\mathbf{f}_s s_s + \sum_{u=0}^{U-1}\sqrt{\frac{P_u G_s}{N_t}}\mathbf{d}_s\mathbf{H}_s\mathbf{F}_u\mathbf{s}_u + \tilde{z}_s, \quad (7)$$

A. OFDM ISAC PROCESSING

The selected method to process the received sensing stream is the one proposed in [7] and used extensively throughout the ISAC literature [13], [14], as well as in the OFDM radar literature [15], typically referred to as symbol domain processing. Considering a case without communication users, we can use (1), (6), (7) with $U = 0$ to represent the signal at the sensing receiver as:

$$\tilde{y}_s = \sqrt{\frac{G_s P_s}{N_t}}\mathbf{d}_s\mathbf{H}_s\mathbf{f}_s s_s + \tilde{z}_s. \quad (8)$$

We can define the OFDM received signal grid matrix using the signal at the sensing receiver from (8) in each symbol and subcarrier of the OFDM grid, i.e., $y_s^{(n,m)}$, as

$$\mathbf{Y}_s = \begin{bmatrix} \tilde{y}_s^{(0,0)} & \cdots & \tilde{y}_s^{(0,M-1)} \\ \tilde{y}_s^{(1,0)} & \cdots & \tilde{y}_s^{(1,M-1)} \\ \vdots & \ddots & \vdots \\ \tilde{y}_s^{(N-1,0)} & \cdots & \tilde{y}_s^{(N-1,M-1)} \end{bmatrix}, \quad (9)$$

where N, M represent the total number of subcarriers and OFDM symbols used.

Similarly, we can define a transmitted OFDM grid, $\mathbf{S}_s$, using the sensing signals transmitted in each symbol and subcarrier of the OFDM grid as

$$\mathbf{S}_s = \begin{bmatrix} s_s^{(0,0)} & \cdots & s_s^{(0,M-1)} \\ s_s^{(1,0)} & \cdots & s_s^{(1,M-1)} \\ \vdots & \ddots & \vdots \\ s_s^{(N-1,0)} & \cdots & s_s^{(N-1,M-1)} \end{bmatrix}. \quad (10)$$

We can perform the element-wise division of the OFDM received grid by the transmitted OFDM grid $\mathbf{S}_s$ to obtain

$$\mathbf{Y} = \mathbf{Y}_s \oslash \mathbf{S}_s = \sqrt{G_s}\begin{bmatrix} \hat{\mathbf{H}}_s^{(0,0)} & \cdots & \hat{\mathbf{H}}_s^{(0,M-1)} \\ \hat{\mathbf{H}}_s^{(1,0)} & \cdots & \hat{\mathbf{H}}_s^{(0,M-1)} \\ \vdots & \ddots & \vdots \\ \hat{\mathbf{H}}_s^{(N-1,0)} & \cdots & \hat{\mathbf{H}}_s^{(N-1,M-1)} \end{bmatrix} + \hat{\mathbf{Z}}_s, \quad (11)$$

where $\hat{\mathbf{Z}}_s$ is the noise matrix after the division, and $\hat{\mathbf{H}}_s = \mathbf{d}_s\mathbf{H}_s\mathbf{f}_s$.

We will consider the point-scatter model for our targets, so G_s is given by

$$G_s = \frac{c_0\sigma_{\mathrm{RCS,t}}}{(4\pi)^3 d_t^4 f_c^2}. \quad (12)$$

The terms c_0, $\sigma_{\mathrm{RCS,t}}$, d_t represent the speed of light, Radar Cross-Section (RCS) of the target and distance to it from the BS, respectively. Moreover, $\hat{\mathbf{H}}_s$ in (11) has elements given by

$$\hat{\mathbf{H}}_s^{(n,m)} = \mathbf{d}_s^{(n,m)}\mathbf{a}_R(\theta_R,\phi_R)\mathbf{a}_T(\theta_T,\phi_T)\cdot e^{j2\pi f_{d,t} m T_0} e^{j2\pi\tau_t(n\Delta f + f_0)}\mathbf{f}_s^{(n,m)}, \quad (13)$$

with $\mathbf{a}_R(\theta_R,\phi_R)$, $\mathbf{a}_T(\theta_T,\phi_T)$ represent the steering vectors at the receiving and transmitting antenna arrays, respectively, in the azimuth θ and elevation ϕ angles of the target. The sensing parameters of interest are the delay τ_t, and Doppler shift $f_{d,t}$, which can be translated to distance and radial velocity as follows

$$d_t = \frac{\tau_t c_0}{2}, \quad (14)$$

$$v_t = \frac{f_{d,t} c_0}{2f_c}. \quad (15)$$

It can be seen from (13) that the estimation of these parameters is equivalent to a spectral estimation problem, so it can be tackled by the use of a two-dimensional periodogram

$$\mathbf{P}_\mathbf{Y} = \frac{1}{NM}\left|\sum_{n=0}^{N_{\mathrm{per}}-1}\left(\sum_{m=0}^{M_{\mathrm{per}}-1}\mathbf{Y}e^{-j2\pi\frac{m}{M_{\mathrm{per}}}}\right)e^{j2\pi\frac{n}{N_{\mathrm{per}}}}\right|^2, \quad (16)$$

In (16), N_{per}, M_{per} represent the length of the periodogram on the fast and slow time axis, respectively. From (16), we obtain a delay-Doppler map on which a Constant False Alarm Rate (CFAR) algorithm can be applied to detect target peaks. A peak detected at location $\mathbf{P}_\mathbf{Y}^{(\hat{n},\hat{m})}$ implies the estimated target's distance and radial velocity given by

$$\hat{d} = \frac{\hat{n}c_0}{2\Delta f N_{\mathrm{per}}}, \quad (17)$$

$$\hat{v} = \frac{\hat{m}c_0}{2f_c T_0 M_{\mathrm{per}}}. \quad (18)$$

Considering the more realistic case where more scatterers would be present, the sensing channel matrix would be modified by the influence of the additional paths. In our analysis, we will consider clutter to be static and targets to be moving (e.g., vehicles), so its differentiation from targets can be done with sufficient resolution on the delay-Doppler map thanks to the clear separation between clutter and targets in the Doppler dimension.

Our analysis of the OFDM processing method in this section so far has only included the sensing stream. However, from (7), we see that in the more relevant case of $U > 0$, we will have interference terms from the communication streams on the sensing receiver. Namely, after applying (11) we will have

$$\mathbf{Y} = \sqrt{\frac{G_s P_s}{N_t}}\hat{\mathbf{H}}_s + \sqrt{G_s}\mathbf{d}_s\mathbf{H}_s\sum_{u=0}^{U-1}\sqrt{\frac{P_u}{N_t}}\hat{\mathbf{S}}_u + \hat{\mathbf{Z}}_s, \quad (19)$$

where $\hat{\mathbf{S}}_u$ is the result of the element-wise division between the precoded OFDM frame for the uth user and the sensing stream. We can see the interference term similar to (7). In the

following section, we introduce the performance metrics to be used and analyze how they are influenced by the presence of interference.

Two assumptions are commonly made when applying the OFDM processing method presented in this section [8]. The first one is that the duration of the Cyclic Prefix (CP) for the OFDM waveform is larger than the round-trip propagation time of the furthermost target. This assumption allows us to disregard the possible effects of Intersymbol Interference (ISI). While authors have considered methods to overcome said ISI [16], we will maintain the assumption to ease our analysis. The second assumption is that the Subcarrier Spacing (SCS) is at least one order of magnitude higher than the largest occurring Doppler shift, preventing Intercarrier Interference (ICI).

B. PERFORMANCE METRICS

Several metrics can be used to evaluate the performance of communications and sensing. For an excellent overview of metrics, the reader can refer to [17]. Our work focuses on the spectral efficiency for communications and the probability of detection p_D together with the CRLB for sensing.

For the spectral efficiency, we can adapt its general expression for the MU-MIMO broadcast channel [18] to include the sensing stream, from which the capacity is obtained by maximizing

$$C_u = \log_2 \det\left(\mathbf{I} + \frac{\mathrm{SNR}_u}{N_t}\mathbf{H}_u\mathbf{F}_u\mathbf{F}_u^*\mathbf{H}_u^*\left(\mathbf{I} + \sum_{j=0,j\neq u}^{U-1}\frac{\mathrm{INR}_j}{N_t}\mathbf{H}_u\mathbf{F}_j\mathbf{F}_j^*\mathbf{H}_u^* + \frac{\mathrm{INR}_s}{N_t}\mathbf{H}_u\mathbf{f}_s\mathbf{f}_s^*\mathbf{H}_u^*\right)^{-1}\right), \tag{20}$$

with

$$\mathrm{SNR}_u = \frac{G_u P_u}{P_n}, \tag{21}$$

$$\mathrm{INR}_j = \frac{G_u P_j}{P_n}, \tag{22}$$

$$\mathrm{INR}_s = \frac{G_u P_s}{P_n}, \tag{23}$$

where P_n represents the noise power. This expression can be extended to multicarrier schemes (e.g., OFDM) by dividing the bandwidth into coherence blocks, but for simplicity, in the rest of the analysis, we will assume flat fading. Starting from (20), we can aim to optimize the sum of spectral efficiencies across all served users as

$$\max_{\mathbf{F}} \sum_{u=0}^{U-1} C_u, \tag{24}$$

where we use $\mathbf{F}$ to represent the set of precoders for all communication users and the sensing stream, including the allocated power to each user

$$\mathbf{F} = \sqrt{\frac{1}{N_t}}\left[\sqrt{P_0}\mathbf{F}_0, \ldots, \sqrt{P_{U-1}}\mathbf{F}_{U-1}, \sqrt{P_s}\mathbf{f}_s.\right] \tag{25}$$

Turning our attention to performance metrics for sensing, we can distinguish two stages with different requirements: target detection, where the goal is to maximize the probability of detection p_D, and target tracking, for which the objective is to obtain a better estimation of the target's parameters, and for that, we want to minimize the CRLB of delay and Doppler shift which are related to distance and velocity respectively. In target detection, a set of scanning beams needs to be planned to cover the entire sensed area, while in target tracking, the beam is pointed toward the previously estimated position of a detected target.

Considering the usage of a CFAR detector [8] in the target detection stage, usually a desired probability of false alarm p_{FA} is set, from which the decision threshold for detecting peaks in the periodogram given by (16) can be obtained. While the statistics of the interference are clearly non-Gaussian, for simplification, we will model the noise plus interference as

$$\tilde{\mathbf{Z}}_{s,i} \sim N_{\mathbb{C}}\left(\mathbf{0}, \sum_{u=0}^{U-1} G_s\mathbf{H}_s\mathbf{F}_u\mathbf{F}_u^*\mathbf{H}_s^* + P_n\mathbf{I}\right), \tag{26}$$

emphasizing that the usage of this model will give, as a result, an upper bound for the threshold. Then, the equation for the threshold is given by

$$\eta_P = -\tilde{P}_n \ln\left(1 - (1 - p_{\mathrm{FA}})^{\frac{1}{N_p M_p}}\right). \tag{27}$$

Here $\tilde{P}_n$ is the total noise-plus-interference power according to (26). Considering the usage of the point scatter model, we will have that a target will cause a periodogram peak at the corresponding bin with height given by

$$\mathbf{P}_{\mathbf{Y}}^{(n_0,m_0)} = NM\sqrt{\frac{P_s}{N_t}}\left(\mathbf{d}_s\mathbf{a}_R(\theta_{R,i},\phi_{R_i})\mathbf{a}_T^*(\theta_{T,i},\phi_{T_i})\mathbf{f}_s\right)\cdot\left(\frac{c_0\sigma_{\mathrm{RCS,t}}}{(4\pi)^3 d_t^4 f_c^2}\right) + \tilde{z}_{s,i}^{(n_0,m_0)}, \tag{28}$$

where $\tilde{z}_{s,i}^{(n_0,m_0)}$ is the noise-plus-interference contribution after passing through the periodogram in (16). Then, the probability of detection can be expressed as

$$p_D = \mathrm{prob}\left(\mathbf{P}_{\mathbf{Y}}^{(n_0,m_0)} > \eta_P\right), \tag{29}$$

with prob$(\cdot)$ denoting a probability. Neglecting the influence of interference of $\tilde{z}_{s,i}(n_0, m_0)$ in (28), which by definition will always be non-negative, we can simplify the analysis by considering the modified periodogram peak height

$$\hat{\mathbf{P}}_{\mathbf{Y}}^{(n_0,m_0)} = NM\sqrt{\frac{P_s}{N_t}}\left(\mathbf{d}_s\mathbf{a}_R(\theta_{R,i},\phi_{R_i})\mathbf{a}_T^*(\theta_{T,i},\phi_{T_i})\mathbf{f}_s\right)\left(\frac{c_0\sigma_{\mathrm{RCS,t}}}{(4\pi)^3 d_t^4 f_c^2}\right). \tag{30}$$

If we consider perfect channel estimation, the only non-deterministic term in (30) is $\sigma_{\text{RCS,t}}$. It is out of the scope of this paper to develop a deep analysis of the RCS, which is by itself a very complex topic [19], [20], [21]. We will assume that a statistical model of $\sigma_{\text{RCS,t}}$ has been derived, with probability density function $f(\sigma_{\text{RCS,t}})$ and cumulative distribution function $F(\sigma_{\text{RCS,t}})$. From it, we can select a value $\hat{\sigma}_{\text{RCS,t}}$ for which the following condition is fulfilled

$$1 - F(\hat{\sigma}_{\text{RCS,t}}) > p_D, \tag{31}$$

and replace it on (30) to plan our sensing accordingly.

Now, for the analysis of the CRLB, we can find the expressions for the distance and velocity estimation [8]

$$\sigma_{\hat{d}} \geq \frac{c_0^2}{\text{SINR}_s(N^2-1)NM(4\pi\Delta f)^2}, \tag{32}$$

$$\sigma_{\hat{v}} \geq \frac{6c_0^2}{\text{SINR}_s(M^2-1)MN(4\pi T_0 f_c)^2}, \tag{33}$$

where $\hat{d}$, $\hat{v}$ are the estimations of distance and velocity. In (32), (33), we have used SINR_s instead of the more traditional SNR applying the same approximation as for the target detection.

From the analysis of (30), (32), (33) we can see that there are fixed system parameters (f_c, Δf, T_0), others that are bound by the bandwidth and transmission time (N, M), and the remaining configurable terms dictate that to maximize p_D and minimize the CRLBs we need to maximize the SINR_s. While in (32), (33) it is obvious, in (30) the dependence is composed by the terms $\sqrt{\frac{P_s}{N_t}}(\mathbf{d}_s\mathbf{a}_R\mathbf{a}_T^*\mathbf{f}_s)$, which directly influence the height of the periodogram peak, and the need to overcome the threshold η_P obtained by (27). This requirement is in symbiosis with the case of communications, where the same is sought to maximize the spectral efficiency, as seen in (20).

We have not included an analysis of the AoA estimation because its estimation is generally done independently of the ISAC processing method and can be obtained through algorithms such as Multiple Signal Classification (MUSIC) [22], [23]. Nevertheless, as seen in [17], its CRLB is also inversely proportional to the SINR_s. Hence, by maximizing SINR_s we can improve all the sensing performance metrics.

III. LINEAR PRECODING AND DECODING FOR ISAC

As the last section clarifies, our goal would be to maximize the SINR for all communication users and the sensing receiver. We propose extending linear precoding techniques typically applied to communications to solve this problem. We will start our analysis with the case of single-antenna users, for which ZF beamforming is used, and later extend the analysis for multi-antenna users, for which BD is applied. For both analisis, we will assume CSIT and that the sensing channel $\mathbf{H}_s$ has also been estimated from the transmission of unprecoded pilots. Additionally, we assume that the sensing direction and, hence, the initial sensing beamformer has been previously obtained either by a beam planning algorithm for the target detection stage or from an initial estimation in the case of target tracking.

A. ZF FOR MISO

ZF beamforming is well-known for the case of the MU Multiple-Input Single-Output (MISO) channel. The procedure includes diagonalizing the channel to all users by applying the Moore-Penrose pseudoinverse as precoding matrix. The addition of sensing requires including the term of the sensing channel associated with a target or a desired sensing direction. Considering the beamforming vector in the direction of the target or sensing direction as $\mathbf{f}_{bs} = \mathbf{a}_T(\theta_T, \phi_T)$, and the U estimations of the channels to each user $\mathbf{h}_u$ with $u \in [0, U-1]$, we form the full channel matrix $\mathbf{H}_a$, given by

$$\mathbf{H}_a = \begin{bmatrix} \mathbf{h}_0 \\ \vdots \\ \mathbf{h}_{U-1} \\ \mathbf{f}_{bs}^* \end{bmatrix}. \tag{34}$$

The non-normalized precoders for each user and the sensing stream would be the columns, $\mathbf{F'}_{a,u}$, of the matrix $\mathbf{F'}_a$ calculated as

$$\mathbf{F'}_a = \mathbf{H}_a^*(\mathbf{H}_a\mathbf{H}_a^*)^{-1}. \tag{35}$$

The normalized precoders $\mathbf{F}_{a,u}$ can be obtained by adjusting each precoder so that their norm is $\sqrt{N_t}$ with

$$\mathbf{F}_{a,u} = \sqrt{N_t}\frac{\mathbf{F'}_{a,u}}{||\mathbf{F'}_{a,u}||}. \tag{36}$$

The term $\mathbf{F}_{a,u}$ represents the uth column of $\mathbf{F}_a$. This way, we guarantee that

$$\mathbf{H}_a\mathbf{F}_a = \begin{bmatrix} \lambda_0 & 0 & \dots & 0 \\ \vdots & \dots & \ddots & \vdots \\ 0 & \dots & \lambda_{U-1} & 0 \\ 0 & \dots & 0 & \lambda_s \end{bmatrix}, \tag{37}$$

where λ_0, λ_s represent the channel gain for the first user and the transmitting gain for the sensing, respectively.

These steps eliminate the interference between streams sent to different communication users and from the sensing stream to them and reduce the reflection of communication streams in the target or sensing location. However, it does not fully remove the interference on the sensing receiver. For this, we need to obtain the equivalent sensing channel to each stream by applying

$$\mathbf{h}_{s,u} = \mathbf{H}_s\mathbf{F}_{a,u}, \tag{38}$$

and form the matrix $\mathbf{H}_{eq,s}$ according to

$$\mathbf{H}_{eq,s} = \begin{bmatrix} \mathbf{h}_{s,0} \\ \vdots \\ \mathbf{h}_{s,U-1} \\ \mathbf{f}_{bs} \end{bmatrix}. \tag{39}$$

We have included $\mathbf{f}_{bs}$ in (39) to account for the path followed by the echoes from the target to the sensing receiver.

Once again, we look for the pseudo-inverse of this equivalent channel, this time following

$$\mathbf{D}'_s = (\mathbf{H}^*_{eq,s}\mathbf{H}_{eq,s})^{-1}\mathbf{H}^*_{eq,s}, \tag{40}$$

which we adjust again following (36) to obtain $\mathbf{D}_s$. Finally, the decoding vector for the communication stream would be given by the last row of $\mathbf{D}_s$, $\mathbf{d}_s$.

The effects of the ZF beamforming can be seen in the performance metrics by doing the appropriate modifications to (20). For the MISO case, we can disregard the interference term and end up with

$$C_u = \log_2\left(1 + \frac{G_u P_u \lambda_u}{N_t P_n}\right). \tag{41}$$

In the case of sensing we would drop the interference term from the assumed noise distribution in (26), which would lower the threshold for target detection in (27) and would allow us to use SNR_s instead of SINR_s in (32), (33).

In terms of complexity, the method is dominated by the calculation of the pseudo-inverse of the aggregate channel matrix, which, assuming an implementation that uses the Singular Vector Decomposition (SVD), is in the order of $\mathcal{O}(N_t^2(U+1))$.

B. BD FOR MIMO

The extension to multi-antenna users is straightforward. One way to implement it would be to consider the multiple channel components of one user to belong to separate users and apply ZF. However, this leaves the burden of reducing interference solely to the transmitter. A more flexible approach is BD, which exploits the fact that the users can apply reception decoders to eliminate intra-user interference [18]. We remind the reader that to simplify the analysis, we will assume that all users have the same number of receiving antennas N_r, and the transmitter sends $N_s = N_r$ streams to each communication user. Starting with the precoder for the uth user, we first form the matrix with the aggregated channels of the rest of the users and the predefined sensing beamformer f_{bs} as

$$\mathbf{H}_{\text{agg}_{\tilde{u}}} = \left[\mathbf{H}_0, \mathbf{H}_1, \ldots, \mathbf{H}_{u-1}, \mathbf{H}_{u+1}, \ldots, \mathbf{H}_{U-1}, \mathbf{f}_{bs}\right]^T. \tag{42}$$

Next, we obtain the SVD of $\mathbf{H}_{\text{agg}_{\tilde{u}}}$ as

$$\mathbf{H}_{\text{agg}_{\tilde{u}}} = \mathbf{U}_{\text{agg}_{\tilde{u}}}\Sigma_{\text{agg}_{\tilde{u}}}[\mathbf{V}^r_{\text{agg}_{\tilde{u}}}\mathbf{V}^n_{\text{agg}_{\tilde{u}}}]^*, \tag{43}$$

in which the basis for the row space of $\mathbf{H}_{\text{agg}_{\tilde{u}}}$, $\mathbf{V}^r_{\text{agg}_{\tilde{u}}}$ are shown separately from the basis of its null space $\mathbf{V}^n_{\text{agg}_{\tilde{u}}}$. Precisely, this $\mathbf{V}^n_{\text{agg}_{\tilde{u}}}$ is the term we want to include in our precoder. With it, we obtain the equivalent channel

$$\mathbf{H}_{\text{eq}_u} = \mathbf{H}_{\text{agg}_{\tilde{u}}}\mathbf{V}^n_{\text{agg}_{\tilde{u}}}. \tag{44}$$

Once again, we use SVD to get

$$\mathbf{H}_{\text{eq}_u} = \mathbf{U}_{\text{eq}_u}\Sigma_{\text{eq}_u}[\mathbf{V}^r_{\text{eq}_u}V^n_{\text{eq}_u}]^*, \tag{45}$$

and to obtain the full precoder we select the basis $\mathbf{V}^r_{\text{eq}_u}$ of the row space of $\mathbf{H}_{\text{eq}_u}$ corresponding to the N_s largest singular values. The final precoder $\mathbf{F}_u$ is obtained as

$$\mathbf{F}_u = \mathbf{V}^n_{\text{agg}_{\tilde{u}}}\mathbf{V}^r_{\text{eq}_u}. \tag{46}$$

The communication decoding vectors, obtained from $\mathbf{U}_{\text{eq}_u}$, should be sent to the receivers for better performance.

For the sensing precoder, we follow the same process, having the aggregated channel of the communication users as the starting point

$$\mathbf{H}_{\text{agg}_s} = \left[\mathbf{H}_0, \mathbf{H}_1, \ldots, \mathbf{H}_{U-1}\right]^T, \tag{47}$$

with SVD given by

$$\mathbf{H}_{\text{agg}_s} = \mathbf{U}_{\text{agg}_s}\Sigma_{\text{agg}_s}[\mathbf{V}^r_{\text{agg}_s}\mathbf{V}^n_{\text{agg}_s}]^*. \tag{48}$$

The difference with the diagonalization process for the communication streams is that we don't want to use the full $\mathbf{H}_s$, but instead direct the energy towards the target or the sensed location. Because of this, we use $\mathbf{f}_{bs}$ as a sort of ideal line-of-sight channel to the target and obtain

$$\mathbf{H}_{eq,s} = \mathbf{f}_{bs}\mathbf{V}^n_{\text{agg}_s}, \tag{49}$$

$$\mathbf{H}_{eq,s} = \mathbf{U}_{eq,s}\Sigma_{eq,s}[\mathbf{V}^r_{eq,s}\mathbf{V}^n_{eq,s}]^*. \tag{50}$$

From the last result we extract the first column of $\mathbf{V}^r_{eq,s}$, which we will represent as $\mathbf{v}_s$, leading to the final sensing stream precoder

$$\mathbf{f}_s = \mathbf{V}^n_{\text{agg}_s}\mathbf{v}_s \tag{51}$$

The procedures explained so far ensure that

$$\mathbf{H}_j\mathbf{F}_u \sim \mathbf{0}, \text{ for } j \neq u, \tag{52}$$

as well as

$$\mathbf{H}_u\mathbf{f}_s \sim \mathbf{0}, \text{ for } u = 0, \ldots, U-1, \tag{53}$$

effectively eliminating interference between the communication users as well as from the sensing stream. In addition, by enforcing (51) we guarantee that there will not be strong reflections from the target containing communication streams. However, we have not dealt with all the interference in the sensing receiver. Similar to the ZF case, we need the sensing channel estimation $\mathbf{H}_s$. With $\mathbf{H}_s$, we can obtain the effective sensing channel for all the communication streams, the $N_t \times U$ matrix $\mathbf{H}_{\text{eff},c}$ given by

$$\mathbf{H}_{\text{eff},c} = \left[\mathbf{H}_s\mathbf{f}_0, \ldots, \mathbf{H}_s\mathbf{f}_{U-1}\right], \tag{54}$$

then apply the SVD to get

$$\mathbf{H}_{\text{eff},c} = [\mathbf{U}^r_{\text{eff},s}\mathbf{U}^n_{\text{eff},s}]\Sigma_{\text{eff},s}\mathbf{V}^*_{\text{eff},s}, \tag{55}$$

after which we end up with the final effective sensing channel, considering only the component from our target or sensing location in the full sensing channel

$$\mathbf{H}_{f,s} = (\mathbf{U}^n_{\text{eff},s})^*\mathbf{a}_R(\theta_{R,i}, \phi_{R_i})\mathbf{a}^*_T(\theta_{T,i}, \phi_{T_i})\mathbf{f}_s. \tag{56}$$

We apply the SVD to get

$$\mathbf{H}_{f,s} = [\mathbf{U}^r_{f,s}\mathbf{U}^n_{f,s}]\Sigma_{f,s}\mathbf{V}_{f,s}, \tag{57}$$

from which we extract the first column from $\mathbf{U}^r_{f,s}$, $\mathbf{u}_s$ and form the final receiver combining vector as

$$\mathbf{d}_s = \mathbf{u}^*_s(\mathbf{U}^n_{f,s})^*. \tag{58}$$

Analyzing the effect of block diagonalization on the spectral efficiency, considering $P_{u,0}, \ldots, P_{u,N_s-1}$ the allocated powers to the N_s streams of the uth user and $\lambda_{u,0}, \ldots, \lambda_{u,N_s-1}$ the singular values of the selected streams, we reach

$$C_u = \sum_{i=0}^{N_s-1} \log_2\left(1 + \frac{G_u P_{u,i}\lambda_{u,i}}{N_t P_n}\right). \tag{59}$$

Since we are considering only one sensing stream, the effect on the sensing performance is similar to what was mentioned in the last subsection.

Comparing the computational complexity with the case of ZF, this time the SVD needs to be performed two times per user, so the computational complexity is in the order of $\mathcal{O}(N_t^2 U(U-1)N_r)$.

C. POWER ALLOCATION FOR ISAC PERFORMANCE OPTIMIZATION

Given the proposed precoding and decoding methods, optimization techniques can be applied to improve the performance of both sensing and communications. Several works can be found where the precoders are directly obtained through solving optimization problems [10], [24]. However, we have already established the procedure for obtaining the precoding and combining vectors, so the optimization must be applied only to find the appropriate power allocation to maximize performance. Despite the difference with prior work, general optimization models as summarized in [25] can be applied:

- Optimize radar performance under communication performance constraints.
- Optimize communication performance under radar performance constraints.
- Optimize the weighted performance of communication and sensing jointly.

We will consider the second option, although modifications to apply the other two strategies are straightforward. As previously mentioned, we will use the sum of spectral efficiency for communication's performance. For sensing, we will use the probability of detection in the case of target detection and the CRLB of distance and velocity in the case of target tracking. The optimization problem can be stated as

$$\begin{aligned} \max_{P_0,P_1,\ldots,P_{U-1},P_s} \quad & \sum_{u=0}^{U-1} C_u \\ \text{s.t.} \quad & \sum_{u=0}^{U-1} P_u + P_s \le P_t \\ & p_D \ge \epsilon_{p_D}, \end{aligned} \tag{60}$$

for target detection, where ϵ_{p_D} is the desired probability of detection. Similarly, for target tracking

$$\begin{aligned} \max_{P_0,P_1,\ldots,P_{U-1},P_s} \quad & \sum_{u=0}^{U-1} C_u \\ \text{s.t.} \quad & \sum_{u=0}^{U-1} P_u + P_s \le P_t \\ & \sigma_{\hat{d}} \ge \epsilon_d \\ & \sigma_{\hat{v}} \ge \epsilon_v, \end{aligned} \tag{61}$$

with ϵ_d, ϵ_v representing the thresholds for the CRLB of distance and velocity respectively. To further simplify the analysis, given that the sensing performance represents a constraint for the optimization problem, we can firstly obtain the required power to meet the sensing requirement by applying (30), (32), (33) accordingly. With this provision, we can solve the remaining optimization for the power allocation of the communication users using water-filling. It is worth noting that we have the RCS as a random variable for the sensing performance. Still, as we mentioned in Section II-B, we can select a value that guarantees that our performance is met with a sufficiently high probability.

IV. USER SELECTION IN MU-MIMO

The application of MU-MIMO for ISAC opens a new problem that has already been extensively covered in the literature for communications: user selection [26], [27], [28], [29]. In a ISAC setup, communications and sensing metrics need to be considered to maximize both functions' performance with the selected user set. In this section, we propose two methods for user selection that build upon existing strategies and add modifications to account for the sensing functionality. We will consider that the system needs to sense in a predefined direction and select the communications users to be served simultaneously. For an overview of user scheduling and user selection strategies, the reader can refer to [30] and [31].

Existing algorithms for user selection in MU-MIMO with linear precoding build upon two main metrics: the gain of the channel and the correlation between different users' channels. In [26], the authors propose an algorithm for user selection with ZF beamforming, which first selects the user that sees the channel with the higher gain and then, iteratively, adds users to the selection by maximizing the sum throughput. In [27], a low-complexity user selection algorithm is proposed that uses the Frobenius norm of the channel as a metric of its achievable capacity. This simplification helps to reduce the number of SVDs required for its implementation, and the authors show that the achieved capacity closely follows the one obtained by exhaustive search. In [28], the authors use the orthogonality of the channels' eigenvectors (related to their correlation) and how large their eigenvalues are to guide the selection process. To reduce the user search space, they propose to define a threshold for the channel eigenvalue, discarding users that

would achieve a lower capacity. All three methods stop if the total number of streams to be transmitted reaches the number of transmitting antennas or if continuing the process would result in a loss of sum capacity.

For extending these methods to ISAC, in addition to considering communication metrics such as capacity or spectral efficiency, we need to include the sensing metrics mentioned in Section II-B. We will aim to maximize the sum spectral efficiency considering the users available for selection while complying with predefined sensing thresholds $\epsilon_{p_D}, \epsilon_d, \epsilon_v$ for the probability of detection, CRLB of the distance, and CRLB of velocity respectively. Drawing inspiration from the methods in [26] and [28], we will also define a threshold for the channel gain ϵ_g to reduce the search space. The channels to a multiple-antenna user will be considered independently and could be added to the selected set individually. We will denote N_u as the total available users, u_n as the user selected on the n-th iteration, Ω as the set of unselected users, and Υ the set of selected users.

We start by forming the matrix $\mathbf{H}_{\text{agg}}$ given by

$$\mathbf{H}_{\text{agg}} = \left[G_0\mathbf{H}_0, \ldots, G_{N_u-1}\mathbf{H}_{N_u-1}, \mathbf{f}_{bs}\right]^T, \tag{62}$$

where we have separated the channel gain from the channel coefficients.

The channel to each user is normalized to having a norm of $N_r N_t$. Each row of $\mathbf{H}_{\text{agg}}$ represents a channel to a user, with the last row being the steering vector to the sensing location.

Next we obtain the fraction P_s of the total transmit power P_t that would need to be allocated to the sensing stream to comply with the sensing performance thresholds, considering as precoder $\mathbf{f}_{bs}$, by applying (30), (32), (33). The initial power allocated to communication streams is given by $P_c = P_t - P_s$. At each iteration, we will select the user that maximizes the sum spectral efficiency and the previously selected users. Additionally, after updating the precoders, we will need to update P_s and P_c. The power allocation within the selected communication users is distributed using water-filling. The selection process, in this case, can be represented as

$$u_n = \max_{u_i \in \Omega_{n-1}} \sum_{\tilde{\Upsilon}_{n,i}} C_{n,i}, \tag{63}$$

where u_n represents the selected user at the n-th iteration, u_i stands for each user in the set Ω_{n-1} of remaining users after $n-1$ iterations, and $\tilde{\Upsilon}_{n,i}$ is the temporary set of selected users formed by adding u_i to the set of selected users Υ_{n-1}.

Alternatively, to reduce the complexity of the search, which requires computing the achievable spectral efficiency for each available user, we could use the correlation between the users' channels. We obtain the correlation matrix $\mathbf{R}_a$, where each element (i, j) is given by

$$\mathbf{R}_a(i, j) = \text{corr}(\mathbf{H}_{\text{agg},i}, \mathbf{H}_{\text{agg},j}), \tag{64}$$

where $\text{corr}(\cdot)$ represents the correlation operation and $\mathbf{H}_{\text{agg},i}, \mathbf{H}_{\text{agg},j}$ are the ith and jth rows of $\mathbf{H}_{\text{agg}}$. At each iteration, the user with the lowest value of $\mathbf{R}_a$ concerning all components in Υ is selected. To take into account the channel gain of the user, we will weight the correlation by the Signal-to-Noise Ratio (SNR) of the user. This selection method can be written as

$$u_n = \min_{i \in \Omega_{n-1}, k \in \Upsilon_{k-1}} \frac{1}{\text{SNR}_i} \sum_{i,k} R_{i,k}. \tag{65}$$

After each iteration, the beampattern gain achievable with the sensing precoder is updated, and the power allocated to the sensing stream is modified accordingly. For both user selection strategies, after the n-th iteration, the resulting sum spectral efficiency C_n is compared to C_{n-1}, and the achievable p_D or CRLB are compared to $\epsilon_{p_D}, \epsilon_d, \epsilon_v$. The process stops if either the capacity decreases or if any of the sensing thresholds are crossed. We can define a terminating condition as

$$T = \begin{cases} 1 & \text{if } C_n > C_{n-1} \wedge \text{(Sensing thresholds kept)}, \\ 0 & \text{if not.} \end{cases} \tag{66}$$

The sensing thresholds are kept if $p_D \geq \epsilon_{p_D} \vee (\sigma_{\tilde{d}} \geq \epsilon_d \wedge \sigma_{\tilde{v}} \geq \epsilon_v)$. Then, the proposed methods can be expressed as in Algorithm 1.

Algorithm 1 Algorithm for User Selection

Require: $\mathbf{H}_{\text{agg}}, \mathbf{R}_a(i, j), \Omega, \Upsilon, P_s, P_c$
Ensure: $\Upsilon_n, P_s, \mathbf{p_c}$
  $C_0 \leftarrow 0$
  $n \leftarrow 1$
  $\Upsilon_0 \leftarrow \Upsilon$
  Obtain $C_n, p_D, \sigma_{\tilde{d}}, \sigma_{\tilde{v}}$
  while $n \leq N_t \wedge T$ **do**
    Select user u_n
    $\Upsilon_n \leftarrow \Upsilon_{n-1} + \{u_n\}$
    $\Omega_n \leftarrow \Omega_{n-1} - \{u_n\}$
    Update $C_n, p_D, \sigma_{\tilde{d}}, \sigma_{\tilde{v}}, P_s$
    $n \leftarrow n + 1$
  end while

In Section V, the performance of both selection strategies will be compared to random user selection and selecting the maximum number of available users. The computational complexity of the two proposed methods can be analyzed by considering ZF as the precoding method. At each iteration, the computational cost is dominated by the need to perform the Moore-Penrose pseudo-inverse, which, considering the SVD-based implementation, has a cost of $\mathcal{O}(N_t^2|\Upsilon_n|)$. In the case of the spectral efficiency-based method, this needs to be performed $|\Omega_n|$ resulting in a computational cost of $\mathcal{O}(N_t^2|\Upsilon_n||\Omega_n|)$. Conversely, for the channel correlation-based method, the pseudo-inverse needs to be calculated only once. If we compare both methods with the exhaustive search, the computational complexity of the latter would be much higher since, at each iteration, the pseudo-inverse

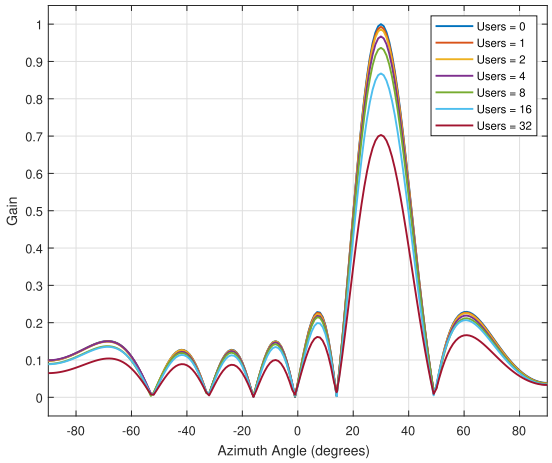

FIGURE 2. Sensing transmitting beampattern.

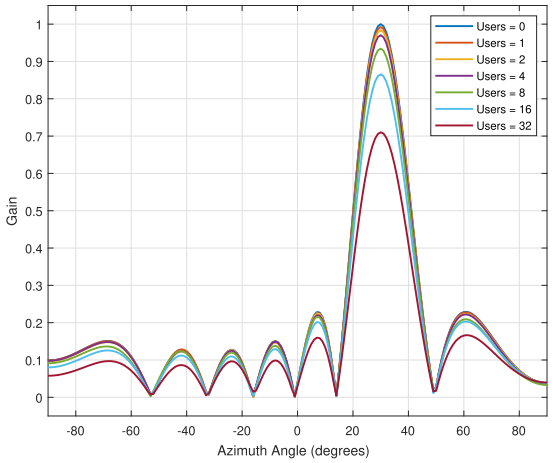

FIGURE 3. Sensing receiving beampattern.

needs to be obtained $\binom{|\Upsilon_n|}{U}$ times. Additional reductions in complexity could be implemented by selecting alternative metrics and precoding strategies. In [32], the reduction of complexity for precoding is studied by using the product of the singular values of the communication users' effective channels as the selection metric and applying the Gram-Schmidt Orthogonalization (GSO) to design the precoders. We believe that the presented methods here are adequate for an initial approach to user selection for ISAC and hope that the field will receive additional contributions in the future with more advanced techniques.

V. SIMULATION RESULTS

To test the proposed methods, we have conducted system simulations with a single small BS, multiple communication users served by that BS, and one target. The BS is equipped with a Uniform Rectangular Array (URA) with 64 antenna elements in a 8×8 configuration. It BS transmits a total power of 43 dBm in the 24 GHz frequency band. We use a Rayleigh fading model to simulate the communication users' channels. Similarly, for the sensing channel, we consider a Rayleigh model to emulate a rich scattering environment and add a component that represents the echo from the target as given by (13).

Firstly, we evaluate the effect of the proposed precoding and decoding methods on the sensing beampattern. We have considered a varying number of communication users and a specific beamforming vector direction, $\mathbf{f}_{\text{bs}}$, of 30° of azimuth and $-15°$ of elevation. Independent channel realizations for each number of users were generated, and no user selection algorithm was applied. The users were assumed to have a single receiving antenna so ZF was applied at the BS. It is worth noting that for the sensing beampattern, the difference between ZF and BD is negligible since there is only one sensing stream, in which both methods result in the same precoder. The results are displayed in Fig. 2 and Fig. 3, where a cut of the beampattern at the elevation angle of $-15°$ is shown. Overall, it can be seen that after applying ZF, the beampattern maintains a high gain at the desired direction even as the number of communication users increases.

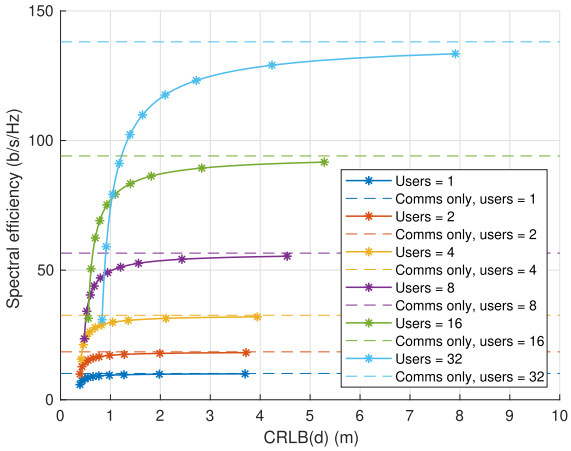

FIGURE 4. Performance trade-offs for ZF.

Next, we tested the effect of varying the power allocation between the communication and sensing functionalities with varying numbers of communication users served. In Figs. 4 and 5, we show the spectral efficiency versus the CRLB of the distance $\sigma_{\tilde{d}}$ for ZF and BD respectively, starting with 90% of the total power allocated to sensing and decreasing it until just 10%. Markers were added at the points where 10, 20, …, 90% of power was allocated to communications. For this simulation, the communication users and the sensing receiver were assumed to have SNRs of 10dB and -40dB, respectively. In the case of BD, users were assumed to have two receiving antennas, resulting in the same number of communication streams to the ZF case. In addition to the trade-off curves, a line with the achievable spectral efficiency for the communications-only scenario was added to the plot.

The figure shows that when increasing the number of served users without modifying the allocated power to each function, sensing performance is affected as expected

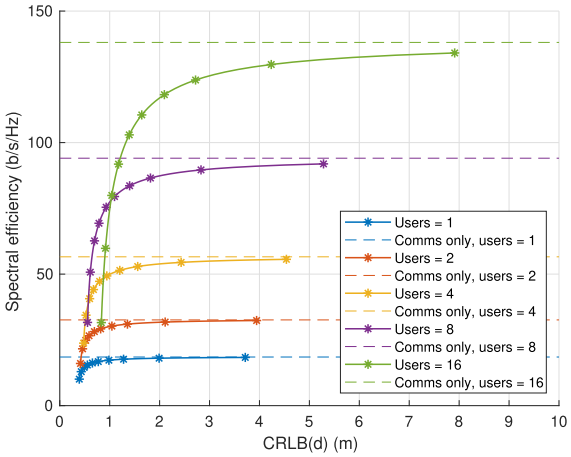

FIGURE 5. Performance trade-offs for BD.

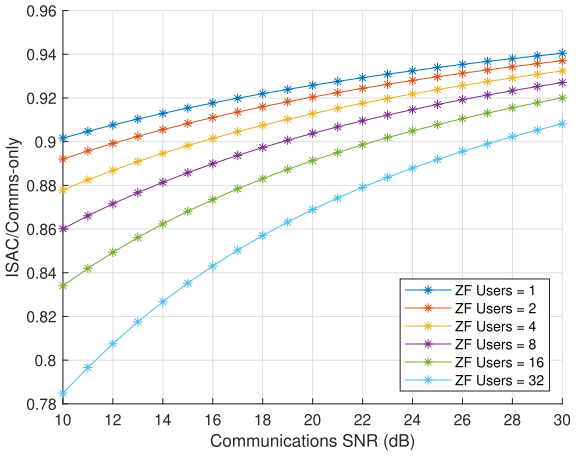

FIGURE 6. Fraction of maximum achievable spectral efficiency reached with ISAC.

due to the loss of beampattern gain. This effect justifies the compensation of power included in the user selection algorithms proposed in Section IV. Additionally, it shows that the spectral efficiency gain at each step decreases when the number of users gradually increases. This is because the power allocated to communications must be distributed among more users. If additional restrictions were to be added, such as a targeted minimum per-user spectral efficiency, changes should be introduced to the user selection mechanism. No significant differences in performance were observed between ZF and BD for the same number of communications streams sent under the simulated conditions.

To further illustrate the gains of the joint operation of communications and sensing, a simulation was conducted with varying values of SNR for the communication users and a fixed power split between communication and sensing of 0.5. The results are shown in Fig. 6 where it can be seen how a significant amount of the communication performance is retained using only half of the transmitting power. Results were shown only for ZF but similar results can be expected for BD. The rest of the simulation parameters were kept the same as for the previous simulations.

Additionally, we ran a simulation in which, taking an initial SNR of -40 dB on the sensing receiver and establishing a reference power split for that value of 0.5, we varied the SNR on the sensing receiver to observe its effect on the spectral efficiency for the communication users, which were simulated with a fixed SNR of 15 dB. As the reader might guess, the simulated variation directly influences the required power split to maintain the sensing performance. In Fig. 7, it can be seen that the effect of varying the sensing SNR is more noticeable for a larger number of users. This behaviour demonstrates the need for precise beamforming and tracking techniques to maximize the performance of both communications and sensing.

Lastly, we tested the proposed user selection strategies, comparing them with two schemes of random user selection. The first one, labelled "Random User Selection" in Fig. 8,

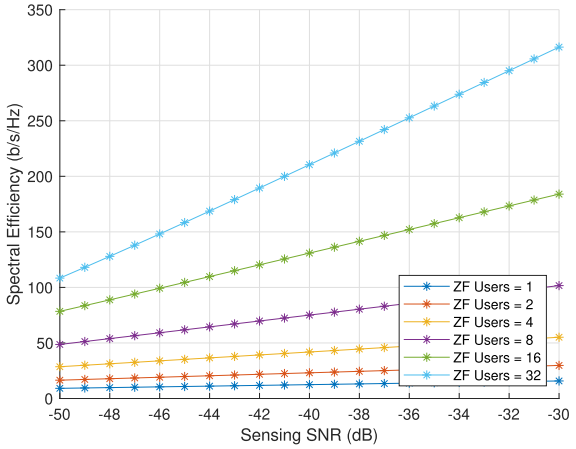

FIGURE 7. Spectral efficiency for varying sensing SNR.

selects a random user from the available user pool in each new iteration as long as communication performance is increased and sensing performance is maintained. The second one, labelled "Maximum Users Selection", starts by selecting the minimum between the total number of users available and the maximum number of users that could be selected given by $N_t - 1$, and removes a random user in each iteration as long as removing that user represents an increase in performance. To evaluate the proposed methods, pools of users were generated in which a percentage of the users could exhibit a high correlation between their channels. A constraint for the sensing performance was set to achieve a $\sigma_{\tilde{d}}$ of 0.5 m. The sum spectral efficiency of the methods proposed in Section IV are compared with random selection in Fig. 8, and the number of users selected for each length of the user pool is shown in Fig. 9.

The results showed that for a small user pool, the spectral efficiency-based user selection method fails to outperform random user selection, with the correlation-based method performing better regarding the sum spectral efficiency and number of users served. When the pool of users is increased,

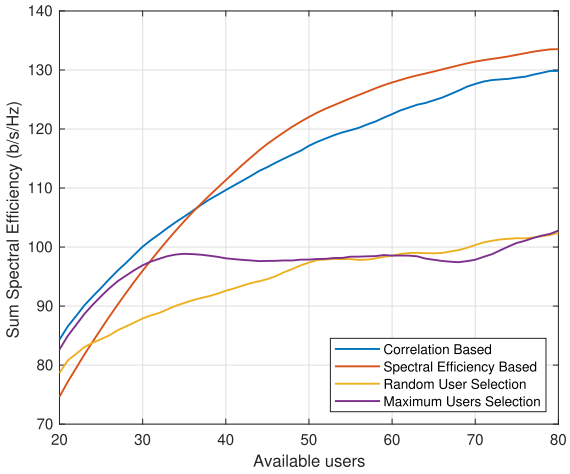

FIGURE 8. Performance trade-offs for ZF.

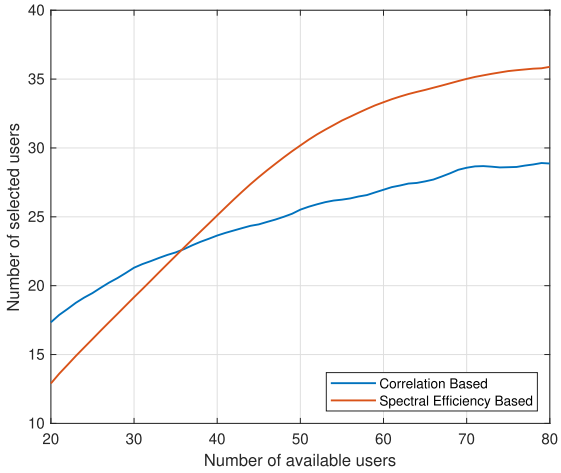

FIGURE 9. Performance trade-offs for BD.

the spectral efficiency-based method catches up with the correlation method in terms of spectral efficiency, slightly outperforming it and achieving a higher number of served users. The random user selection fails to use large user pools to increase performance, justifying user selection techniques to improve spectral efficiency without compromising sensing performance.

VI. CONCLUSION

In this paper, we showed the applicability of two linear precoding and decoding techniques, namely ZF beamforming and BD, to ISAC in a MU-MIMO scenario. The extension of both techniques to ISAC was made possible by adding a sensing channel estimation, effectively treating the sensing receiver as another user. The extensions of the precoding techniques to eliminate the interference in the sensing receiver were presented. The simulation results showed that the multiuser interference was handled without compromising the sensing performance, maintaining a beampattern gain of 70% of the reference beamformer in both transmitter and receiver while serving 32 communications streams. No significant differences between ZF and BD regarding performance were observed, leaving the decision of which to use as an implementation preference. Moreover, the effects of varying the power allocation between the two functionalities in their performance metrics were shown. While the strategy followed here aimed to maximize communication performance and maintain the sensing metrics above predefined thresholds, different approaches could lead to alternative solutions for resource allocation and could be an object of further study. Additionally, two user selection strategies were proposed and proved superior to arbitrary user selection, especially for large user pools. For future work, we expect to add the usage of IBFD for both communications and sensing and explore the effect of errors in the sensing channel estimation on the sensing performance. Additionally, we plan to study the possible benefits of using echoes from the communication streams for sensing.

ACKNOWLEDGMENT

The authors want to thank the reviewers for their helpful comments. For Fig. 1, elements made by macrovector for freepik.com were used.

REFERENCES

[1] F. Liu, C. Masouros, A. P. Petropulu, H. Griffiths, and L. Hanzo, "Joint radar and communication design: Applications, state-of-the-art, and the road ahead," *IEEE Trans. Commun.*, vol. 68, no. 6, pp. 3834–3862, Jun. 2020, doi: 10.1109/TCOMM.2020.2973976.

[2] F. Liu, Y. Cui, C. Masouros, J. Xu, T. X. Han, Y. C. Eldar, and S. Buzzi, "Integrated sensing and communications: Toward dual-functional wireless networks for 6G and beyond," *IEEE J. Sel. Areas Commun.*, vol. 40, no. 6, pp. 1728–1767, Jun. 2022, doi: 10.1109/JSAC.2022.3156632.

[3] H. Wymeersch, D. Shrestha, C. M. de Lima, V. Yajnanarayana, B. Richerzhagen, M. F. Keskin, K. Schindhelm, A. Ramirez, A. Wolfgang, M. F. de Guzman, K. Haneda, T. Svensson, R. Baldemair, and S. Parkvall, "Integration of communication and sensing in 6G: A joint industrial and academic perspective," in *Proc. IEEE 32nd Annu. Int. Symp. Pers., Indoor Mobile Radio Commun. (PIMRC)*, Oulu, Finland, Sep. 2021, pp. 1–7.

[4] T. Wild, V. Braun, and H. Viswanathan, "Joint design of communication and sensing for beyond 5G and 6G systems," *IEEE Access*, vol. 9, pp. 30845–30857, 2021.

[5] D. K. Pin Tan, J. He, Y. Li, A. Bayesteh, Y. Chen, P. Zhu, and W. Tong, "Integrated sensing and communication in 6G: Motivations, use cases, requirements, challenges and future directions," in *Proc. 1st IEEE Int. Online Symp. Joint Commun. Sens.*, Dresden, Germany, Feb. 2021, pp. 1–6.

[6] J. A. Zhang, Md. L. Rahman, K. Wu, X. Huang, Y. J. Guo, S. Chen, and J. Yuan, "Enabling joint communication and radar sensing in mobile networks—A survey," *IEEE Commun. Surveys Tuts.*, vol. 24, no. 1, pp. 306–345, 1st Quart., 2022, doi: 10.1109/COMST.2021.3122519.

[7] C. Sturm, T. Zwick, and W. Wiesbeck, "An OFDM system concept for joint radar and communications operations," in *Proc. IEEE 69th Veh. Technol. Conf.*, Barcelona, Spain, Apr. 2009, pp. 1–5, doi: 10.1109/VETECS.2009.5073387.

[8] M. Braun, "OFDM radar algorithms in mobile communication networks," Ph.D. thesis, Karlsruher Inst. Technol., Karlsruhe, Germany, 2014.

[9] F. Liu, L. Zhou, C. Masouros, A. Li, W. Luo, and A. Petropulu, "Toward dual-functional radar-communication systems: Optimal waveform design," *IEEE Trans. Signal Process.*, vol. 66, no. 16, pp. 4264–4279, Aug. 2018, doi: 10.1109/TSP.2018.2847648.

[10] F. Liu, Y.-F. Liu, A. Li, C. Masouros, and Y. C. Eldar, "Cramér-Rao bound optimization for joint radar-communication beamforming," *IEEE Trans. Signal Process.*, vol. 70, pp. 240–253, 2022, doi: 10.1109/TSP.2021.3135692.

[11] X. Liu, T. Huang, and Y. Liu, "Transmit design for joint MIMO radar and multiuser communications with transmit covariance constraint," *IEEE J. Sel. Areas Commun.*, vol. 40, no. 6, pp. 1932–1950, Jun. 2022, doi: 10.1109/JSAC.2022.3155512.

[12] C. B. Barneto, S. D. Liyanaarachchi, T. Riihonen, L. Anttila, and M. Valkama, "Multibeam design for joint communication and sensing in 5G new radio networks," in *Proc. IEEE Int. Conf. Commun. (ICC)*, Dublin, Ireland, Jun. 2020, pp. 1–6, doi: 10.1109/ICC40277.2020.9148935.

[13] L. Pucci, E. Paolini, and A. Giorgetti, "System-level analysis of joint sensing and communication based on 5G new radio," *IEEE J. Sel. Areas Commun.*, vol. 40, no. 7, pp. 2043–2055, Jul. 2022, doi: 10.1109/JSAC.2022.3155522.

[14] C. Baquero Barneto, T. Riihonen, M. Turunen, L. Anttila, M. Fleischer, K. Stadius, J. Ryynänen, and M. Valkama, "Full-duplex OFDM radar with LTE and 5G NR waveforms: Challenges, solutions, and measurements," *IEEE Trans. Microw. Theory Techn.*, vol. 67, no. 10, pp. 4042–4054, Oct. 2019, doi: 10.1109/TMTT.2019.2930510.

[15] C. Knill, F. Embacher, B. Schweizer, S. Stephany, and C. Waldschmidt, "Coded OFDM waveforms for MIMO radars," *IEEE Trans. Veh. Technol.*, vol. 70, no. 9, pp. 8769–8780, Sep. 2021, doi: 10.1109/TVT.2021.3073268.

[16] K. Wu, J. A. Zhang, X. Huang, and Y. J. Guo, "Integrating low-complexity and flexible sensing into communication systems," *IEEE J. Sel. Areas Commun.*, vol. 40, no. 6, pp. 1873–1889, Jun. 2022, doi: 10.1109/JSAC.2022.3156649.

[17] A. Liu, Z. Huang, M. Li, Y. Wan, W. Li, T. X. Han, C. Liu, R. Du, D. K. P. Tan, J. Lu, Y. Shen, F. Colone, and K. Chetty, "A survey on fundamental limits of integrated sensing and communication," *IEEE Commun. Surveys Tuts.*, vol. 24, no. 2, pp. 994–1034, 2nd Quart., 2022, doi: 10.1109/COMST.2022.3149272.

[18] R. W. Heath Jr. and A. Lozano, *Foundations of MIMO Communication*, 1st ed., Cambridge, U.K.: Cambridge Univ. Press, 2018.

[19] C. Uluisik, G. Cakir, M. Cakir, and L. Sevgi, "Radar cross section (RCS) modeling and simulation, Part 1: A tutorial review of definitions, strategies, and canonical examples," *IEEE Antennas Propag. Mag.*, vol. 50, no. 1, pp. 115–126, Feb. 2008, doi: 10.1109/MAP.2008.4494511.

[20] T. Schipper, J. Fortuny-Guasch, D. Tarchi, L. Reichardt, and T. Zwick, "RCS measurement results for automotive related objects at 23–27 GHz," in *Proc. 5th Eur. Conf. Antennas Propag. (EUCAP)*, Roma, Italy, Apr. 2011, pp. 683–686.

[21] I. Matsunami, N. Ryohei, and A. Kajiwara, "Target state estimation using RCS characteristics for 26GHz short-range vehicular radar," in *Proc. Int. Conf. Radar*, Sep. 2013, pp. 304–308, doi: 10.1109/RADAR.2013.6652003.

[22] Y. L. Sit, C. Sturm, J. Baier, and T. Zwick, "Direction of arrival estimation using the MUSIC algorithm for a MIMO OFDM radar," in *Proc. IEEE Radar Conf.*, Atlanta, GA, USA, May 2012, pp. 0226–0229, doi: 10.1109/RADAR.2012.6212141.

[23] Z. Cheng and B. Liao, "QoS-aware hybrid beamforming and DOA estimation in multi-carrier dual-function radar-communication systems," *IEEE J. Sel. Areas Commun.*, vol. 40, no. 6, pp. 1890–1905, Jun. 2022, doi: 10.1109/JSAC.2022.3155529.

[24] Z. Wang, K. Han, X. Shen, W. Yuan, and F. Liu, "Achieving the performance bounds for sensing and communications in perceptive networks: Optimal bandwidth allocation," *IEEE Wireless Commun. Lett.*, vol. 11, no. 9, pp. 1835–1839, Sep. 2022, doi: 10.1109/LWC.2022.3183235.

[25] X. Liu, T. Huang, F. Liu, Z. Zheng, Y. Liu, and Y. C. Eldar, *Joint Precoding Design for Multi-Antenna Multi-User ISAC Systems*. Singapore: Springer, 2023, pp. 211–240.

[26] G. Dimic and N. D. Sidiropoulos, "On downlink beamforming with greedy user selection: Performance analysis and a simple new algorithm," *IEEE Trans. Signal Process.*, vol. 53, no. 10, pp. 3857–3868, Oct. 2005, doi: 10.1109/TSP.2005.855401.

[27] Z. Shen, R. Chen, J. G. Andrews, R. W. Heath, and B. L. Evans, "Low complexity user selection algorithms for multiuser MIMO systems with block diagonalization," *IEEE Trans. Signal Process.*, vol. 54, no. 9, pp. 3658–3663, Sep. 2006, doi: 10.1109/TSP.2006.879269.

[28] A. Bayesteh and A. K. Khandani, "On the user selection for MIMO broadcast channels," *IEEE Trans. Inf. Theory*, vol. 54, no. 3, pp. 1086–1107, Mar. 2008, doi: 10.1109/TIT.2007.915887.

[29] S. Huang, H. Yin, J. Wu, and V. C. M. Leung, "User selection for multiuser MIMO downlink with zero-forcing beamforming," *IEEE Trans. Veh. Technol.*, vol. 62, no. 7, pp. 3084–3097, Sep. 2013, doi: 10.1109/TVT.2013.2244105.

[30] D. Sabat, P. Pattanayak, A. Kumar, and G. Prasad, "A contemporary review on user scheduling techniques and feedback reduction strategies towards the development of 5G and beyond communications," *Phys. Commun.*, vol. 58, Jun. 2023, Art. no. 102070, doi: 10.1016/j.phycom.2023.102070.

[31] E. Castañeda, A. Silva, A. Gameiro, and M. Kountouris, "An overview on resource allocation techniques for multi-user MIMO systems," *IEEE Commun. Surveys Tuts.*, vol. 19, no. 1, pp. 239–284, 1st Quart., 2017, doi: 10.1109/COMST.2016.2618870.

[32] M. Al-Shuraifi, "Transmit antenna selection and user selection in multiuser MIMO downlink systems," Ph.D. thesis, Brunel Univ. London, Middlesex, U.K., 2016.

CARLOS RAVELO (Graduate Student Member, IEEE) received the B.S. degree in electronics and communications from the Technical University of Havana, in 2015. He is currently pursuing the Ph.D. degree in telecommunications with the Polytechnic University of Valencia as part of the ITN-5VC Project within the MSCA Actions.

DAVID MARTÍN-SACRISTÁN received the Ph.D. degree in telecommunications engineering from the Universitat Politècnica de València (UPV), Spain, in 2016. From 2006 to 2020, he was a Researcher with the ITEAM Research Institute, UPV. Since 2020, he has been the Chief Technology Officer with 5G Communications for Future Industry Verticals and an Adjunct Professor with the Universitat de València. His research interests include modeling and simulation of communication networks, beyond 5G, the IoT, and vehicular communications.

JOSE F. MONSERRAT (Senior Member, IEEE) is currently a Full Professor and the Vice President of the Universitat Politècnica de València, the first technical university in Spain. He has been involved in several European projects, such as METIS/METIS-II where he led the simulation activities, or currently 5G-CARMEN and 5GSMART. He co-edited the books *Mobile and Wireless Communications for IMT-Advanced and Beyond* (Wiley) and *5G Mobile and Wireless Communications Technology* (Cambridge University Press). He has published more than 60 journal articles. His research team comprises five postdoctoral fellows, eight Ph.D. students, and two master's students. He has served as the European Parliament and the World Bank Group Advisor in the vehicular 5G communications topic. His research interests include the design of beyond 5G wireless systems and their performance assessment.